Transient nonlinear electrical transport of hot electrons in nonpolar semiconductors

Deug Yong Kim and Chang Sub Kim*
Department of Physics, Chonnam National University, Kwangju, 500-757 Korea
(Received 1 July 1994; revised manuscript received 18 January 1995)

The transient transport of charged carriers is studied theoretically using the Boltzmann kinetic equation in nonpolar semiconductors limited by acoustic deformation potential scattering in the presence of steady electric fields. The conventional two-term approximation in the Legendre polynomial expansion is employed for solutions to the Boltzmann equation for optically generated hot electrons. The resulting time-dependent Boltzmann-Fokker-Planck equation is numerically solved for the isotropic distribution function by utilizing a matrix method. The subsequent relaxation of the nonequilibrium hot carriers toward a steady state is watched as time elapses for the pulsed initial conditions. It is seen that the solution tends to the well-known nonequilibrium steady Davydov-Druyvesteyn distribution function at an infinite-time limit. The obtained time-dependent solutions are used to calculate the drift velocities of carriers, thus the transient electron mobilities, and also the hot electron temperatures for various field strengths. In addition, the decay of the electron temperature and mobility is analyzed in terms of an effective transient relaxation time. The noticeable advantages of our numerical matrix method are as follows: it is very efficient in time, and its interpretation of outcome is direct, in that the reciprocal of the smallest non-zero eigenvalue of the Boltzmann-Fokker-Planck operator corresponds to the characteristic relaxation time.

I. INTRODUCTION

The semiclassical Boltzmann equation is a widely used theoretical tool in investigating the electrical transport properties of semiconductors.[1,2] Since the density of carriers in semiconductors, which are responsible for transporting charge, momentum, and energy, can be made sufficiently low in most circumstances, a consideration of uncorrelated two-body scattering is reasonable for an effective description of many-body dynamics. For such a low density system the statistical description in terms of the one particle distribution function is particularly useful and the Boltzmann equation is a well-established kinetic equation for determination of the nonequilibrium distribution function, including an understanding of its limitation in the space and time scales under consideration. Once the distribution function is determined, physically interesting macroscopic properties and transport coefficients can be calculated. On the other hand, it is still quite a difficult task to solve it, in general because of its mathematical nature as an integro-differential equation and also because of physical constraints such as the complex band structures as well as the various scattering mechanisms.

Among the various methodologies of solving the Boltzmann equation we pay attention to the *sp approximation* whose earlier appearances are in literature such as the work of Yamashita and Watanabe[3] and Levinson,[4] subsequently in others,[1,2,5] and also which has been treated recently by several investigators.[6–9] When the considered semiconductor material is under the influence of the steady electric fields, the cylindrical symmetry is induced in the direction along the field. Then, when the scattering process involved is isotropic, it seems reasonable to expand the solution to the Boltzmann equation in terms of the complete Legendre polynomials with the angle defined between the direction of the electric field and the momentum of an electron. The conventional two-term approximation or *sp* approximation takes only two terms in the expansion, assuming that the isotropic distribution function is dominant over other angle-dependent terms. Thus the *sp* approximation should be useful when a quasielastic scattering is dominant so that the role of the scattering is to randomize the direction of electron momentum.[10] Here, one should notice that the expansion is not a perturbation in the electric field, instead it appears as an external parameter in this formalism. Thus the validity of the *sp* approximation goes beyond the Ohmic regime to some extent. It is well known that electron–acoustic-phonon scattering is quasielastic and is a dominant scattering mechanism in intrinsic nonpolar semiconductors such as Ge and Si at low temperatures.[1,11] Consequently, the aforementioned methodology of solving the Boltzmann equation has been applied to these materials frequently in evaluating the momentum and energy relaxation time and transport coefficients such as the mobility. However, most workers have restricted their interest to the steady-state calculation and it is rare to obtain the time-dependent solution. This is presumably because the resulting differential equation of the *sp* approximation is still quite complicated to solve under time-dependent condition and also because most physical interest in the previous works was restricted to the steady-state properties. However, with the development of extremely short laser pulses and its application to the spectroscopy it becomes possible to experimentally study various transport properties in the transient regime.[12–15] Then, it becomes an increasingly important endeavor to investigate the relaxation of the nonequilibrium distribution of optically excited electrons

 ©1995 The American Physical Society

and their approach to equilibrium theoretically and thus to calculate transient transport coefficients which are important characteristics in device application.

This work presents the time-dependent solution of the Boltzmann equation within the *sp* approximation, applying to a single-valley semiconductor that has some relevance to nonpolar semiconductors under the influence of the external stationary electric field. We adopt for our calculations the material parameters of Ge, whose electric-field dependence of drift velocity and electron mobility in the steady state is well known.[16–18] We restrict our attention to transport by a single type of carrier, optically excited electrons which are assumed to be nondegenerate. Initially, the electrons are injected into a particular conduction state and thus the electron distribution function at later times shows a transient behavior and eventually relaxes to the steady state via acoustic deformation potential scattering, which in turn approaches the equilibrium Maxwell-Boltzmann distribution function in the zero-field limit.

In the Boltzmann equation approach for transport calculations, specifying the energy band structure and the scattering mechanisms are prerequisite. Here we specify our semiconductor such that electron–acoustic-phonon scattering is the dominant scattering mechanism and only an effective single spherical valley is considered for the energy band. An argument for the validity of the specifications is as follows. In general, for nonpolar semiconductor electron–optical-phonon and electron–acoustic-phonon scattering, electron-impurity scattering, and also electron-electron scattering are involved. The electron-impurity scattering is important for doped semiconductors at low temperatures, however, it may not be considered for optically excited pure semiconductors. And, we do not include electron-electron scattering, assuming that the density of excited electrons is sufficiently small. The optical-phonon scattering is not treated either since it is small compared to electron-acoustic phonon scattering in nonpolar materials at low temperatures. For band structures we adopt the single parabolic band with spherical constant energy surface according to the usual observation that the spherical model is sufficient for semiconductors with cubic symmetry although, for instance, Ge has four equivalent valleys. This simplification is also motivated by the recent temporal Monte Carlo result, where it is reported that the simple Si model with a single spherical and parabolic band and a simplified scattering mechanism generates accurate electron velocity and electron energy up to intermediate applied fields.[19]

Our goal is to provide the time-dependent solution to the Boltzmann equation within the *sp* approximation and thus to study the transient transport properties of optically injected hot electrons limited by long wavelength acoustic phonons. The resulting differential equation of the *sp* approximation is named the Boltzmann-Fokker-Planck (BFP) equation since the differential operator derived resembles the Fokker-Planck operator. The steady-state solution to this problem was previously derived and treated by other authors in a similar context.[1,2,6] On the other hand, the time-dependent solution has not been obtained before. We treat the problem as an eigenvalue problem: we first solve the eigenvalue equation for the BFP operator and expand the initial distribution function in terms of the eigenvectors obtained, then the solution at a later time is written formally as sums of exponential terms with the exponent of time weighted by the eigenvalues. In doing so, the essential ingredient of our approach is to obtain an approximate Hilbert space where the nonequilibrium distribution function is written. Without knowing the exact eigenfunctions of the BFP operator the usual technique is to expand the solution in terms of some special orthonormal polynomials so as to approximately represent the physical operator as a matrix. Although this method is expected to arrive at the solution faster than the commonly used Monte Carlo numerical scheme,[20] still it is an extensive numerical diagonalization procedure, since the desired accuracy is dependent on the number of expanding basis functions. We optimize this procedure by the unitary transformation from the polynomial basis to the quadrature basis.[21] Then, the resultant matrix representation of the Boltzmann-Fokker-Planck operator in the quadrature basis is diagonalized. In this case, the necessary order of matrix for the desired accuracy, equivalently the number of expanding polynomials, is only a few tens. The method of solving the FP equation by expansion into a complete set is also discussed in Ref. 22. The prominent advantages of our numerical matrix method are as follows: it is very efficient in time, and the interpretation of its outcome is direct: if the eigenvalue spectrum of the BFP operator is discrete the reciprocal of the smallest nonzero eigenvalue would correspond to the characteristic relaxation time. Since it is a continuing research interest to develop a faster and more efficient numerical method of solving the transport equation,[23–25] this work may serve as an alternative in investigating the transient transport problems in semiconductors.

The paper is organized as follows. In Sec. II, the conventional two-term approximation for a solution to the Boltzmann equation is reviewed in order to clarify the various approximations taken and thus to understand its physical implication, and also in order to provide the derivation of the BFP equation which is the working basis of our transport calculation. The numerical matrix method that we have utilized in solving the BFP eigenvalue problem is presented in Sec. III. The results and discussions are provided in Sec. IV. Finally, a summary is given in Sec. V.

II. THE BOLTZMANN-FOKKER-PLANCK EQUATION

In this section we develop an approximate differential equation whose solution specifies the nonequilibrium distribution function of the excited electrons, starting from the semiclassical Boltzmann equation. It is well known that the Boltzmann equation can be transformed into a Fokker-Planck equation when an appropriate coarse graining is taken in energy space.[9,26,27] We consider a model semiconductor in which the transport carriers are nondegenerate electrons that are created by an incoher-

ent optical pumping and that are assumed to interact with only long wavelength acoustic phonons via deformation potential scattering under the influence of stationary electric fields.

Then, the Boltzmann equation to be considered is

$$\frac{\partial f(\vec{k},t)}{\partial t} - \frac{e\vec{E}}{\hbar}\cdot\frac{\partial f(\vec{k},t)}{\partial \vec{k}} = J[f] \tag{1}$$

where the collision integral $J[f]$ is given by

$$J[f] = \int \frac{d\vec{k}'}{(2\pi/L)^3}\left[S(\vec{k},\vec{k}')f(\vec{k}',t) - S(\vec{k}',\vec{k})f(\vec{k},t)\right]. \tag{2}$$

In the above e is the absolute value of the electron charge and $\vec{E}$ is the static external electric field applied to the semiconductor with one dimensional size L. The collision operator $J[f]$ is linear in the distribution function f because carrier-carrier scattering is not considered. Also, $S(\vec{k},\vec{k}')$ specifies the transition rate of the electron being scattered from a state $|\vec{k}'\rangle$ to another state $|\vec{k}\rangle$ by emitting or absorbing a phonon within a parabolic energy band. As usual, we look for the expansion solution to Eq. (1) in terms of the Legendre polynomial and take the two-term ansatz[3,4] as

$$f(\vec{k},t) = f^{(0)}(\varepsilon_k,t) + kf^{(1)}(\varepsilon_k,t)\cos\theta\ , \tag{3}$$

where θ is the angle between the electric field and the electron wave vector $\vec{k}$. The constant energy surface is specified as

$$\varepsilon_k = \hbar^2k^2/2m^* \tag{4}$$

for the effective single spherical valley model with m^* being the effective mass of the electron. In the expansion Eq. (3) the first term represents the isotropic part of the distribution function and the second term specifies the anisotropic contribution. Here, one notices that the ansatz naturally incorporates the physical constraint that the drift velocity is much smaller than the thermal velocity. The transition rate at a long-time limit is determined by the Fermi golden rule and can be written, as for the present case,

$$S(\vec{k},\vec{k}') = \frac{2\pi}{\hbar}A(q)\left\{\begin{matrix} n_q \\ n_q+1\end{matrix}\right\}\delta(\varepsilon_{k'} - \varepsilon_k \pm \hbar\omega_q), \tag{5}$$

where the plus sign corresponds to the absorption of a phonon and the minus sign indicates the emission of a phonon in the collision process. In the above $\vec{q}$ is the momentum transfer, $\vec{q} = \vec{k} - \vec{k}'$, assuming no umklapp process. Also, n_q is the thermal average occupancy of phonons in the mode ω_q, that is, $n_q = 1/[\exp(\hbar\omega_q/k_BT_0) - 1]$ and $\hbar\omega_q$ is the energy of one phonon. The hot phonon effect is not considered in the current work, thus phonons remain in equilibrium at temperature T_0 and play the role as a heat reservoir. For the considered acoustic deformation potential scattering

$$A(q) = \hbar E_1^2 q/2L^3\rho c_s, \tag{6}$$

where c_s is the speed of longitudinal waves, ρ is the mass density of ions, and E_1 is the deformation potential constant.[28]

Then, by substituting Eqs. (3) and (5) into Eq. (1), and choosing the positive z as the direction of the electric field, and also by making use of the orthogonality of the Legendre polynomials, one can obtain a set of coupled equations as

$$\frac{\partial f^{(0)}(\varepsilon_k,t)}{\partial t} - \frac{eE}{\hbar}\left\{f^{(1)}(\varepsilon_k,t) + \frac{2}{3}\varepsilon_k\frac{\partial f^{(1)}}{\partial\varepsilon_k}\right\} = J[f^{(0)}] \tag{7}$$

and

$$\frac{\partial f^{(1)}(\varepsilon_k,t)}{\partial t} - \frac{eE\hbar}{m^*}\frac{\partial f^{(0)}}{\partial\varepsilon_k} = J[f^{(1)}], \tag{8}$$

where the expressions for $J[f^{(0)}]$ and $J[f^{(1)}]$ are given in Ref. 27.

In the low-field approximation it is expected that the distribution function only slightly deviates from the equilibrium Boltzmann distribution function. In fact, it can be easily seen that the collision integral vanishes in Eq. (7) when $f^{(0)} \propto \exp(-\varepsilon_k/k_BT_0)$ is substituted. Since the second term in the left side of Eq. (7) contributes only as higher order effects, it can be concluded that Eq. (7) admits the Boltzmann distribution function as a correct equilibrium solution. Then, one can obtain a self-contained equation for $f^{(1)}$ from Eq. (8) and can proceed to solve it. This is the frequently used linearized Boltzmann equation approach in the literature.[29,30]

On the other hand, it is an increasingly important effort to study the high-field transport in semiconductors.[31–34] In this case, even the isotropic part of the solution at long times is not to be presumed to be the Maxwell-Boltzmann distribution function. Instead, that must be determined by solving Eq. (7). In this case Eq. (7) is not self-contained. This difficulty is circumvented by the very assumption that the second term $f^{(1)}$ in the expansion Eq. (3) is much smaller than the first term,[4] and thus the variation of $f^{(1)}$ in time as well as energy is negligible in the sense that it is at least one order less significant compared to $f^{(1)}$. In other words, the initial anisotropy of distribution function induced by the applied field quickly diminishes due to the quasielastic isotropic electron-phonon scattering in our model. Also, because the energy of acoustic phonons is small compared to that of electrons at temperatures considered, $\hbar\omega_q \ll \varepsilon_k$, the off-diagonal terms of $f^{(0)}$ and $f^{(1)}$ in Eqs. (7) and (8) are expanded in terms of $\hbar\omega_q/\varepsilon_k$. In addition, we take the energy equipartition approximation, $n_q + 1 \approx n_q \approx k_BT_0/\hbar\omega_q$, which is valid because the acoustic-phonon frequency is low for temperatures ~ 100 K. Finally, the phonon dispersion relation is specified as $\omega_q = c_sq$ in the long wavelength limit.

Then, by taking all these into account one can obtain a self-contained equation for $f^{(0)}$ and the result is

$$\frac{\partial f^{(0)}(x,t^*)}{\partial t^*} = \frac{1}{\sqrt{x}}\frac{\partial}{\partial x}\left[(x^2-2x-\alpha)+\frac{\partial}{\partial x}(x^2+\alpha x)\right] \times f^{(0)}(x,t^*) , \quad (9)$$

where the dimensionless variables x and t^* are defined to be

$$x \equiv \frac{\varepsilon_k}{k_B T_0}, \quad t^* \equiv t/\tau_0 , \quad (10)$$

where the constants α and τ_0 are given in Ref. 27. Further, we find it useful to define

$$g^{(0)}(x,t^*) \equiv \sqrt{x} f^{(0)}(x,t^*). \quad (11)$$

Then, Eq. (9) becomes

$$\frac{\partial g^{(0)}(x,t^*)}{\partial t^*} + \tilde{L} g^{(0)}(x,t^*) = 0 \quad (12)$$

in which the linear differential operator $\tilde{L}$ is defined to be

$$\tilde{L} = -\frac{\partial}{\partial x}\left[a(x)+\frac{\partial}{\partial x}b(x)\right] , \quad (13)$$

where

$$a(x) = (x^2-2x-\alpha)/\sqrt{x}, \quad b(x) = (x^2+\alpha x)/\sqrt{x}. \quad (14)$$

One recognizes that the differential operator $\tilde{L}$ takes the form of the familiar Fokker-Planck operator.[22] Since Eq. (12) has been derived from the Boltzmann equation, it is called the Boltzmann-Fokker-Planck equation. A similar Fokker-Planck equation was derived recently by Cavalleri and Mauri for systems with an electron-electron interaction in the presence of an electric field.[9]

The steady-state solution for Eq. (12) is obtained from

$$a(x)\sqrt{x} f^{(0)}(x) + \frac{\partial}{\partial x}\left[b(x)\sqrt{x} f^{(0)}(x)\right] = 0 , \quad (15)$$

where the first term represents the drift flux induced by the electric field and the second term represents the diffusion flux in energy space due to the electron–acoustic-phonon collision. Since the sedimentation equilibrium is reached when the diffusion flux compensates the drift flux, the total flux is required to vanish in the long-time limit. Blatter and co-workers discussed the competing aspects of acceleration and deceleration of the carriers due to the electric field and the scattering with phonons by a Fokker-Planck equation in energy space.[26] By integrating Eq. (15) one can obtain

$$f^{(0)}(x) = \frac{C}{\sqrt{x} b(x)} \exp\left[-\int^x dx' a(x')/b(x')\right] = C(x+\alpha)^{\alpha} e^{-x} , \quad (16)$$

where the integration constant C is determined from the conservation of the number of particles. Here one recognizes that the steady solution $f^{(0)}(x)$ is the well-known Davydov distribution function of electron gas under steady electric field. Also, one can notice that $f^{(0)}(x)$ approaches the equilibrium Maxwell-Boltzmann distribution $\propto \exp(-x)$ as $E \to 0$, which confirms that the BFP equation produces the correct equilibrium solution. In contrast, it is seen that the distribution function $f^{(0)}(x)$ behaves as $\exp(-x^2/2\alpha)$ in the limit of very strong fields, which is known as the Druyvesteyn distribution function.[35] Recently, evidence for a Druyvesteyn energy distribution in hot electron electroluminescence was reported.[36] Also, a generalization of the distribution function Eq. (16) was obtained by Liboff and Schenter incorporating degenerate effects.[6]

III. NUMERICAL MATRIX METHOD

The numerical analysis that we have used for solutions to the BFP equation is described in this section. The BFP operator plays a role as the generator of time translation for the distribution function. Thus, if the eigenfunctions and eigenvalue spectrum of the BFP operator are obtained, the time-dependent solution is formally determined by causing the BFP operator to act on the initial distribution function that is specified as an expansion in terms of the eigenfunctions. Particularly, when the eigenvalue spectrum is discrete, it can be expressed as a sum of exponential terms with exponents of time weighted by eigenvalues. For this purpose, we find it useful to normalize the distribution function $g^{(0)}(x,t^*)$ with respect to the steady-state solution $f^{(0)}(x)$ as

$$\Phi(x,t^*) \equiv \frac{g^{(0)}(x,t^*)}{\sqrt{x} f^{(0)}(x)} \quad (17)$$

so that Φ will become unity as the system approaches the steady state. Then, the BFP equation (12) is rewritten as

$$\frac{\partial \Phi(x,t^*)}{\partial t^*} + \hat{L}(x)\Phi(x,t^*) = 0 , \quad (18)$$

where the linear differential operator $\hat{L}$ is newly defined to be

$$\tilde{L} \to \hat{L} \equiv D^{-1}(x)\tilde{L} f^{(0)}(x) = a(x)\frac{\partial}{\partial x} - b(x)\frac{\partial^2}{\partial x^2}. \quad (19)$$

Hereafter, we will omit the asterisk in denoting time and it should be understood to be dimensionless according to Eq. (10) without confusion. The solution to Eq. (18) can be formally expanded in terms of the complete eigenvectors of the operator $\hat{L}$ as

$$\Phi(x,t) = e^{-\hat{L}t}\Phi(x,0) = \sum_{n=0}^{\infty} \alpha_n e^{-\lambda_n t}\eta^{(n)}(x) , \quad (20)$$

where the eigenvalue λ_n and eigenvector $\eta^{(n)}(x)$ are subjected to the eigenvalue equation

$$\hat{L}\Phi(x) = \lambda\Phi(x). \quad (21)$$

In Eq. (20) the expansion coefficients α_n are to be specified from the initial distribution of optically generated

conduction electrons. The above eigenvalue problem can be treated by employing the polynomial expansion method:

$$\Phi(x) = \sum_n c_n \phi_n(x), \tag{22}$$

where the associated Laguerre polynomials with weight function $w(x) = xe^{-x}$ are chosen for the complete orthonormal polynomials $\{\phi_n(x)\}$ in the relevant domain of x.[38] Then, the eigenvalue equation is written in the Hilbert space spanned by *the polynomial basis* $\{c_n\}$ as

$$\sum_j \hat{L}_{ij}^{(p)} c_j = \lambda c_i , \tag{23}$$

where the matrix representation of the operator $\hat{L}$ is given by

$$\hat{L}_{ij}^{(p)} = \int_0^\infty dx\, \phi_i(x) \hat{L} \phi_j(x). \tag{24}$$

In order to obtain the desired accuracy a large number of polynomials in the expansion that corresponds to the dimension of the matrix to be diagonalized is usually required, which makes the numerical investigation very extensive. In the current work we employ a discrete ordinate method that provides an effective numerical scheme of discretization of the BFP operator at the set of optimally chosen energy points. This optimization procedure is essentially equivalent to the Gaussian quadrature rule where a relatively small number of points accurately represent an integration. This is done by rotating the polynomial basis into *the quadrature basis* $\{\hat{\Phi}_i\}$ according to

$$\hat{\Phi}_i = \sum_j U_{ji} c_j , \tag{25}$$

where the transformation is unitary and it is given as

$$U_{ij} = \phi_i(\xi_j)\sqrt{\chi_i} , \tag{26}$$

where $\{\xi_i\}$ and $\{\chi_i\}$ are the quadrature abscissas and weights, respectively, determined by the Gauss-Laguerre rule. The details of this method have been reported recently in Ref. 21. Then, the eigenvalue equation (36) is written in the quadrature basis as

$$\sum_l \hat{L}_{ij}^{(q)} \hat{\Phi}_j = \lambda \hat{\Phi}_i , \tag{27}$$

where the matrix representation of the operator $\hat{L}$ in the quadrature basis is obtained by the similarity transformation

$$\hat{L}_{ij}^{(q)} = \sum_{l,m} U_{il}^\dagger \hat{L}_{lm}^{(p)} U_{mj} . \tag{28}$$

The result is given as

$$\hat{L}_{ij}^{(q)} = a(\xi_i) D_{ij}^{(q)} - b(\xi_i) \sum_l D_{il}^{(q)} D_{lj}^{(q)} , \tag{29}$$

where

$$D_{ij}^{(q)} = \sum_n \sqrt{\chi_i} U_{nj} \frac{d\phi_n(\xi_i)}{dx}. \tag{30}$$

In the above, the matrix representation of the operator $\hat{L}$ obtained is not symmetric, accordingly neither the reality of the eigenvalues nor the orthogonality of the eigenvectors is guaranteed. This is because the operator $\hat{L}$ is not self-adjoint in the Hilbert space spanned by $\{\phi_n\}$. However, it is possible to construct a new Hilbert space in which the transformed BFP operator is self-adjoint with respect to the new weight function, $P_0(x) \equiv \sqrt{x} f^{(0)}(x)$. The new orthonormal complete basis $\{\psi_n\}$ is given as

$$\psi_n(x) \equiv \sqrt{\frac{w(x)}{P_0(x)}} \phi_n(x). \tag{31}$$

Then, one can evaluate the matrix element of the operator $\hat{L}$ in the newly defined polynomial basis such that

$$\begin{aligned}\int_0^\infty dx\, P_0(x)\psi_i(x)\hat{L}\psi_j(x) &= -\int dx\, \psi_i(x) \left[\frac{\partial}{\partial x}[a(x)P_0(x)\psi_j(x)] + \frac{\partial^2}{\partial x^2}[b(x)P_0(x)\psi_j(x)]\right] \\ &= \int_0^\infty dx\, P_0(x) b(x) \psi_i'(x) \psi_j'(x) ,\end{aligned} \tag{32}$$

where integration by parts has been used in the last step with vanishing $P_0(x)$ at $x = 0$ and ∞. The result clearly shows that the matrix representation is symmetric in the newly defined Hilbert space. Due to the connection between two polynomial bases, Eq. (31), one can expect that the matrix representation, Eq. (32), would be the matrix representation of a different self-adjoint operator in the $\{\phi_n\}$ basis. In fact, this turns out to be the case as is seen in the following:

$$\begin{aligned}\int_0^\infty dx\, P_0(x)\psi_i(x)\hat{L}\psi_j(x) &= \int_0^\infty dx\, P_0(x) \sqrt{\frac{w(x)}{P_0(x)}} \phi_i(x) \\ &\quad \times \hat{L}\left(\sqrt{\frac{w(x)}{P_0(x)}}\phi_j(x)\right) \\ &= \int dx\, w(x)\phi_i(x)\hat{M}\phi_j(x) ,\end{aligned} \tag{33}$$

where the new self-adjoint operator has been defined to be

$$\hat{M} \equiv \sqrt{\frac{P_0(x)}{w(x)}} \cdot \hat{L} \cdot \sqrt{\frac{w(x)}{P_0(x)}}. \tag{34}$$

Thus the matrix element of the operator $\hat{M}$ in the polynomial basis $\{\phi_n\}$ is defined as

$$\hat{M}_{ij}^{(p)} = \int dx\ w(x)b(x)\left[\phi_i'(x) + p(x)\phi_i(x)\right] \times \left[\phi_j'(x) + p(x)\phi_j(x)\right] , \tag{35}$$

where

$$p(x) \equiv \frac{1}{2}\left(\frac{w'(x)}{w(x)} - \frac{P_0'(x)}{P_0(x)}\right). \tag{36}$$

We evaluate the above integration by utilizing the N-point Gaussian quadrature to obtain

$$\begin{aligned}\hat{M}_{ij}^{(p)} &= \sum_{n=0}^{N-1} \chi_n b(\xi_n)\left[\phi_i'(\xi_n) + p(\xi_n)\phi_i(\xi_n)\right] \times \left[\phi_j'(\xi_n) + p(\xi_n)\phi_j(\xi_n)\right] \\ &= \sum_{k,l,n} b(\xi_n)U_{ik}U_{jl}\left[D_{nk}^{(q)} + p(\xi_k)\delta_{nk}\right] \times \left[D_{nl}^{(q)} + p(\xi_l)\delta_{nl}\right] ,\end{aligned} \tag{37}$$

which clearly manifests the symmetry in interchanging the indices i, j. Then, the quadrature representation can be obtained by performing the similarity transformation, and the result is

$$\begin{aligned}\hat{M}_{ij}^{(p)} \to \hat{M}_{ij}^{(q)} &= \sum_{m,q}\left[U_{im}^t \hat{M}_{mq}^{(p)} U_{qj}\right] \\ &= \sum_{n=0}^{N-1} b(\xi_n)\left[D_{ni}^{(q)} + p(\xi_n)\delta_{ni}\right] \times \left[D_{nj}^{(q)} + p(\xi_n)\delta_{nj}\right].\end{aligned} \tag{38}$$

Therefore the problem is finally reduced to solving the well-defined eigenvalue problem

$$\hat{M}_{ij}^{(q)}\Psi_j^{(\mu)} = \lambda_\mu \Psi_j^{(\mu)}\delta_{ij} , \tag{39}$$

where λ_μ is the μth eigenvalue and $\Psi_j^{(\mu)}$ is the jth component of the μth eigenvector. Once the eigenvalue problem is solved, the time-dependent distribution function is obtained at the discretized energy points $\{\xi_i,\ i = 0, \ldots, N-1\}$ according to

$$\hat{\Phi}(\xi_i, t) = \sum_{\mu=0}^{N-1} c_\mu e^{-\lambda_\mu t}\sqrt{\frac{w(\xi_i)}{P_0(\xi_i)}}\Psi_i^{(\mu)} , \tag{40}$$

where the coefficients c_μ are determined from the initial condition. In the long-time limit the solution should admit the known steady distribution function as a solution, which means that the smallest eigenvalue must be zero. Then, the steady-state distribution function is calculated from

$$\hat{\Phi}(\xi_i, t \to \infty) = \sqrt{\frac{w(\xi_i)}{P_0(\xi_i)}} c_0 \Psi_i^{(0)} , \tag{41}$$

the value of which is unity according to the normalization Eq. (17).

IV. RESULTS AND DISCUSSIONS

We have solved the BFP equation by utilizing the matrix method that is presented in the preceding section. Consequently, the time-dependent distribution functions have been obtained for nonequilibrium electrons that were assumed to be injected into a conduction band by incoherent optical excitation. Then, the relevant transport properties have been evaluated and analyzed in the transient regime under the various physical conditions in detail. The results are presented here.

The material parameters that we have adopted for the current calculations are the ones appropriate for Ge at $T_0 = 100$ K:[37]

$$\begin{aligned} m^* &= 0.2m_e, \\ \rho &= 5.35\ \text{g/cm}^3, \\ c_s &= 5.4 \times 10^5\ \text{cm/sec}, \\ E_1 &= 9.5\ \text{eV}. \end{aligned}$$

The electron mean free path evaluated from these parameters according to Ref. 27 is given as $l_{ac} \doteq 5.6 \times 10^{-5}$ cm and the characteristic time τ_0 is determined to be $\tau_0 \doteq 0.59$ nsec. The eigenvalues in the formal solution, Eq. (40), are in units of τ_0^{-1} and the energy points $\{\xi_i\}$ are in units of $k_B T_0 \doteq 8.6 \times 10^{-3}$ eV.

The smallest eigenvalue of the matrix representation of the BFP operator must be zero, as mentioned earlier, because of the condition of particle conservation. Thus the accuracy of our numerical calculation is strictly dependent upon the satisfaction of this requirement. However, the satisfactory value of the smallest eigenvalue is not obtained by simply increasing the order of matrix. Instead, the goal was achieved by introduction of the rescaling factor s in the formulation according to

$$x \to x' = \frac{1}{s}x , \tag{42}$$

where $s \equiv T/T_0$. By doing so, we freely normalize the energy with respect to some other temperature T different from the equilibrium T_0. It turns out that the rescaling of energy becomes important with an increase of the applied field. A larger scale factor means that effectively more quadrature points are placed in the high energy region. For this purpose, we replace x by sx' in the formulas, for instance, the symmetrized matrix representation of $\hat{L}$ is written as

$$\hat{M}_{ij}^{(q)} = \frac{1}{\sqrt{s}}\sum_{n=0}^{N-1} b(s\xi_n)\left[D_{ni}^{(q)} + p(s\xi_n)\delta_{ni}\right] \times \left[D_{nj}^{(q)} + p(s\xi_n)\delta_{nj}\right] , \tag{43}$$

where

$$p(sx') = \frac{2(s-1)x'^2 + (1-2\alpha/s)x' + \alpha/s}{4x'(x'+\alpha/s)}, \quad (44)$$

$$b(sx') = \frac{1}{\sqrt{x'}}\left(x'^2 + \frac{\alpha}{s}x'\right). \quad (45)$$

The optimal value of s for a given E and N has been determined by trial and error until the smallest eigenvalue reaches zero as shown in Table I, where the eigenvalue spectrum of the BFP operator is given for a field of $E = 1.0 \times 10^4$ V/m using the number of expansion polynomials (or, equivalently the number of optimally chosen energy points) of $N = 25$. It shows that the eigenvalue spectrum is discrete at least for a few of the lowest values. The exact dependence of the eigenvalue on the scaling parameter is expected to be complicated and is not given here as a functional form, however, it is possible to obtain such a desirable value. In a separate calculation it has been seen that for a fixed N the value of the optimum scaling parameter that produces the desired λ_0 becomes larger as the magnitude of the electric field increases. This means that more points are sampled in the high energy region in order to accurately represent the distribution function under the high-field condition.

The steady-state distribution function $f^{(0)}(x)$ is obtained at the discretized energies according to

$$\sqrt{\xi_i} f^{(0)}(s\xi_i) = \frac{1}{\chi_i}\omega(\xi_i)\left[\Psi_i^{(0)}\right]^2. \quad (46)$$

The result is given in Fig. 1 for the various magnitudes of the field but for a fixed N, where the electron population is normalized to unity for convenience. In the figure the squares represent the numerically obtained data and the solid lines are the analytical result from Eq. (16). The numerical outcome coincides with the analytic result, which demonstrates clearly the effectiveness of the current numerical scheme: only a small amount of numerical data represents the steady-state distribution function correctly, $N = 15$ in this case. The role of the parameter s is observed to be placing more points optimally in the high energy region in the higher-field case, compared to the result of the smaller field for a fixed N. Also, it is seen that more electrons are occupied in the high energy state when the applied fields are stronger, which means the average electron energy is bigger for large fields compared to that of the smaller field case.

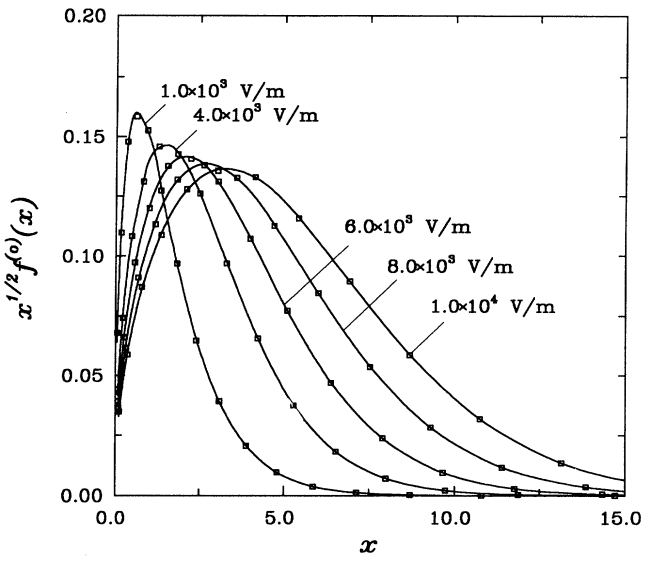

FIG. 1. Average electron population in the steady state for several electric fields with a fixed $N = 15$ at $T_0 = 100$ K; the solid lines are the results from the analytic Davydov distribution $\sqrt{x}f^{(0)}(x)$ and the centered symbols (□) indicate the data obtained from the numerical matrix method $w(\xi_j)\left[\Psi_j^{(0)}\right]^2 / \chi_j$.

Since we are interested in incoherent relaxation of the energy distribution function, here no attention is paid to the actual optical generation processes of the initial hot electron distribution. In other words, the initial condition should not matter in the time scale we consider. Accordingly, we have chosen the pulsed initial condition as a simple model, assuming that all excited electrons are pumped into a particular conduction state $x = s\xi_m$,

$$f^{(0)}(s\xi_l, t=0) = N_0\delta_{lm}, \quad (47)$$

where δ_{lm} is the Kronecker delta function and N_0 specifies the total number of the excited electrons N_e according to

TABLE I. Dependence of the eigenvalues on the scale factor s; $E = 1.0 \times 10^4$ V/m and $N = 25$.

s	λ_0	λ_1	λ_2	λ_5	λ_{10}
1.00000[−2][a]	5.7655[+1]	3.0483[+2]	7.5028[+2]	3.3665[+3]	1.2930[+4]
1.10000[−1]	7.7392[−1]	9.2249[+0]	2.4006[+1]	1.0984[+2]	4.1280[+2]
2.40000[−1]	3.7330[−3]	4.5697[+0]	1.0719[+1]	4.2519[+1]	1.5164[+2]
3.00000[−1]	4.0905[−5]	4.4873[+0]	1.0143[+1]	3.4951[+1]	1.1736[+2]
3.20100[−1]	2.2036[−7]	4.4838[+0]	1.0103[+1]	3.3480[+1]	1.0944[+2]
3.22500[−1]	1.8602[−9]	4.4836[+0]	1.0101[+1]	3.3332[+1]	1.0858[+2]
3.22251[−1]	7.1844[−11]	4.4836[+0]	1.0101[+1]	3.3347[+1]	1.0867[+2]
3.22293[−1]	9.7842[−14]	4.4836[+0]	1.0101[+1]	3.3345[+1]	1.0866[+2]

[a] $[\pm n] \equiv 10^{\pm n}$.

$$N_e(t=0) = s\int_0^\infty dx' D(sx') f^{(0)}(sx',0)$$
$$= s\sum_l \chi_l \omega^{-1}(\xi_l) D(s\xi_l) f^{(0)}(s\xi_l,0) \ , \qquad (48)$$

where $D(x)$ is the density of states that equals $2VN_c\sqrt{x}/\sqrt{\pi}$ in which N_c is the effective density of states that is defined to be $(m^* k_B T/\pi\hbar^2)^{3/2}/\sqrt{2}$. Then, the subsequent relaxation of the electron distribution function is completely specified by Eq. (40) where the expansion coefficients c_μ are determined by the initial condition $\Phi(s\xi_l,0) = f(s\xi_l,0)/f^{(0)}(s\xi_l)$. The result is written as

$$\Phi(s\xi_l,t) = \frac{N_e(0)}{D(s\xi_m)f^{(0)}(s\xi_m)}\left[\frac{P_0(s\xi_m)}{P_0(s\xi_l)}\frac{\omega(\xi_l)}{\omega(\xi_m)}\right]^{1/2}$$
$$\times \frac{\omega(\xi_m)}{s\sqrt{\chi_m\chi_l}}\sum_\mu e^{-\lambda_\mu t}\Psi_l^{(\mu)}\Psi_m^{(\mu)}. \qquad (49)$$

It can be proved easily that Eq. (49) satisfies the chosen initial condition by making use of the orthonomality condition $\sum_\mu \Psi_l^{(\mu)}\Psi_m^{(\mu)} = \delta_{lm}$. In order to demonstrate the relaxation of the initially sharply peaked electron distribution toward a steady state we find it convenient to define the ratio of the distribution function with respect to the steady result as

$$\Phi^*(s\xi_j,t) \equiv \Phi(s\xi_j,t)/\Phi(s\xi_j,t=\infty)$$
$$= \frac{1}{\Psi_j^{(0)}\Psi_m^{(0)}}\sum_{\mu=0}^{N-1} e^{-\lambda_\mu t}\Psi_j^{(\mu)}\Psi_m^{(\mu)} \ , \qquad (50)$$

which tends to unity at long times. The result is drawn in Fig. 2 for a low field $E = 5.0 \times 10^2$ V/m at various time steps calculated with $N = 15$. In Fig. 2(a) electrons are initially pumped into the energy $x \doteq 0.9$ and in Fig. 2(b) $x \doteq 4.6$. A smooth line has been drawn through the data points (□), although the distribution function is evaluated at the discretized energies. The initially sharply peaked distribution function at the injected energy broadens with time and approaches the steady-state distribution at infinite time. The portion of the curves below unity indicates an underpopulation of carriers with respect to the steady-state distribution and the portion above unity represents an overpopulation. It shows that electrons excited at a higher energy relax slowly compared to the low excitation result due to the fact that it should emit more phonons before reaching the steady state. The same features are seen in Fig. 3 for a much higher field of strength $E = 5 \times 10^4$ V/m for two initial conditions evaluated with $N = 35$; $x \doteq 30$ in Fig. 3(a) and $x \doteq 49$ in Fig. 3(b). The initially δ-function-like pumped electron distributions are significantly depopulated already within a time scale of tens of picoseconds.

Once the distribution function is determined, the macroscopic thermodynamic states of the electron gas such as the total number of excited electrons, the hot electron temperature, and the drift velocity can be calculated by taking proper moments over the distribution function. In particular, the number of electrons should remain constant in time since neither recombination process nor trapping are considered in the current calculation. We have checked the condition of particle conservation at each time utilizing the following expression in order to monitor the numerical accuracy:

$$N_e^*(t) \equiv N_e(t)/N_e(0)$$
$$= \sum_{l=0}^{N-1}\left[\left(\frac{\chi_l^2\xi_m}{\chi_m^2\xi_l}\right)^{1/4}\left(\frac{s\xi_l/\alpha+1}{s\xi_m/\alpha+1}\right)^{\alpha/2}\right.$$
$$\left.\times\sqrt{\frac{e^{(s-1)\xi_m}}{e^{(s-1)\xi_l}}}\sum_\mu e^{-\lambda_\mu t}\Psi_l^{(\mu)}\Psi_m^{(\mu)}\right] \qquad (51)$$

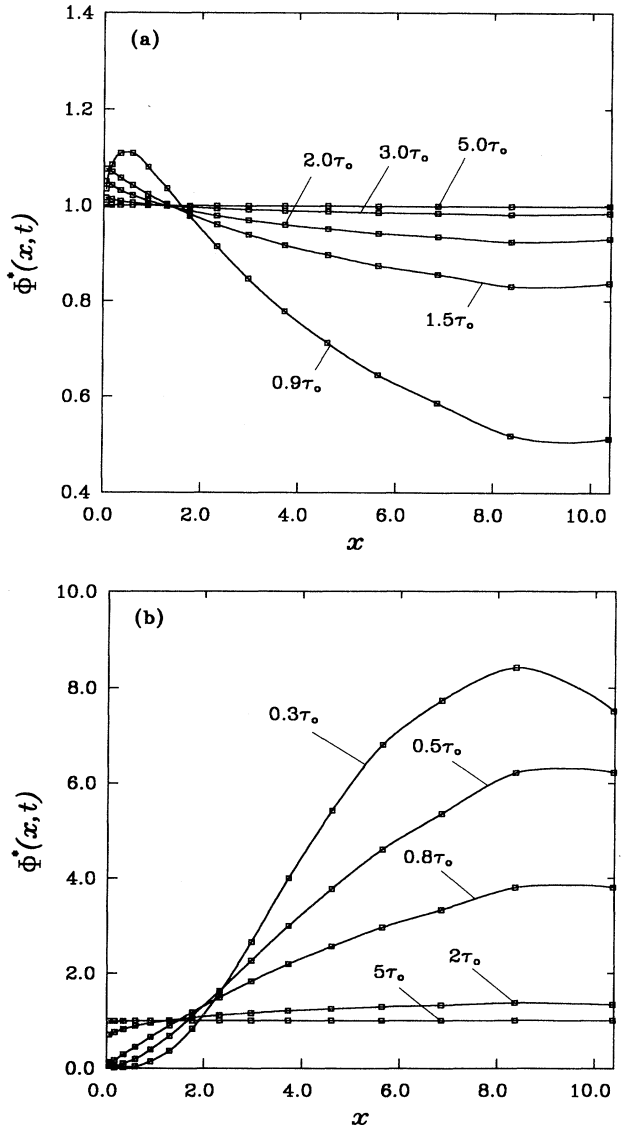

FIG. 2. Relaxation of the time-dependent distribution function $\Phi^*(x,t) = \Phi(x,t)/\Phi(x,\infty)$ at several times in units of $\tau_0 = 0.59$ nsec for an electric field $E = 5 \times 10^2$ V/m at $T_0 = 100$ K; the electrons are initially peaked at (a) $x \doteq 0.9$; (b) $x \doteq 4.6$, where x is in units of $k_B T_0 \doteq 8.6 \times 10^{-3}$ eV. The symbols (□) indicate the values of the distribution function at the discretized energy points.

and the result was quite satisfactory that the calculation produced $N_e^*(t) = 1$ at all times.

Next, we define the hot electron temperature $T_e(t)$ to be the average electron energy evaluated by the time-dependent distribution function obtained according to

$$\frac{3}{2}k_B T_e(t) = k_B T_0 s^2 \int_0^\infty dx' D(sx')x' f(sx', t). \quad (52)$$

Here, we find it convenient to normalize the electron temperature with respect to the equilibrium T_0 as $T_e^*(t) \equiv T_e(t)/T_0$, for which the expression is given as

$$T_e^*(t) = T_e^*(\infty) + \sum_{\mu=1}^{N-1} \alpha_\mu \exp(-\lambda_\mu t), \quad (53)$$

where $T_e^*(\infty)$ is the steady-state electron temperature and

$$\alpha_\mu = \frac{2}{3}s \sum_{l=0}^{N-1} \left[\xi_l \left\{ \frac{\chi_l \sqrt{\xi_m}(s\xi_l/\alpha + 1)^\alpha e^{(s-1)\xi_m}}{\chi_m \sqrt{\xi_l}(s\xi_m/\alpha + 1)^\alpha e^{(s-1)\xi_l}} \right\}^{1/2} \times \Psi_l^{(\mu)} \right] \Psi_m^{(\mu)}. \quad (54)$$

The relaxation of the nonequilibrium electron temperature corresponding to the distribution functions in Figs. 2 and 3 is shown in Figs. 4 and 5, respectively, including several additional initial conditions. The electrons are accelerated toward the opposite of the direction of the applied field, which results in an increase of average electron energy in time. This gain of energy is compensated by the electron's loss of energy through scattering with acoustic phonons. Thus, before reaching the sedimentation equilibrium, electrons are either heated up or cooled down depending on the initial excitation condition. These transient effects are clearly manifested in the results. In Fig. 4 it is seen that the initial electron temperature $T_e^*(0)$ heats up when the electron temperature at $t = 0$ is lower than the steady hot temperature $T_e^*(\infty)$ and it cools down when $T_e^*(0)$ is higher than $T_e^*(\infty)$. For the chosen low field of $E = 5 \times 10^2$ V/m the hot electron temperature in the steady state is close to T_0, $T_e^*(\infty) \doteq 1.03$, which is independent of the initial excitation conditions. The same features are shown for a high field, $E = 5.0 \times 10^4$ V/m in Fig. 5 where the steady hot temperature is determined to be $T_e^*(\infty) \doteq 15.4$. In Fig. 6 another illustration is given of transient behavior of the decay of the electron temperature with changing of the magnitude of applied fields for a fixed initial condition $x \doteq 4.6$

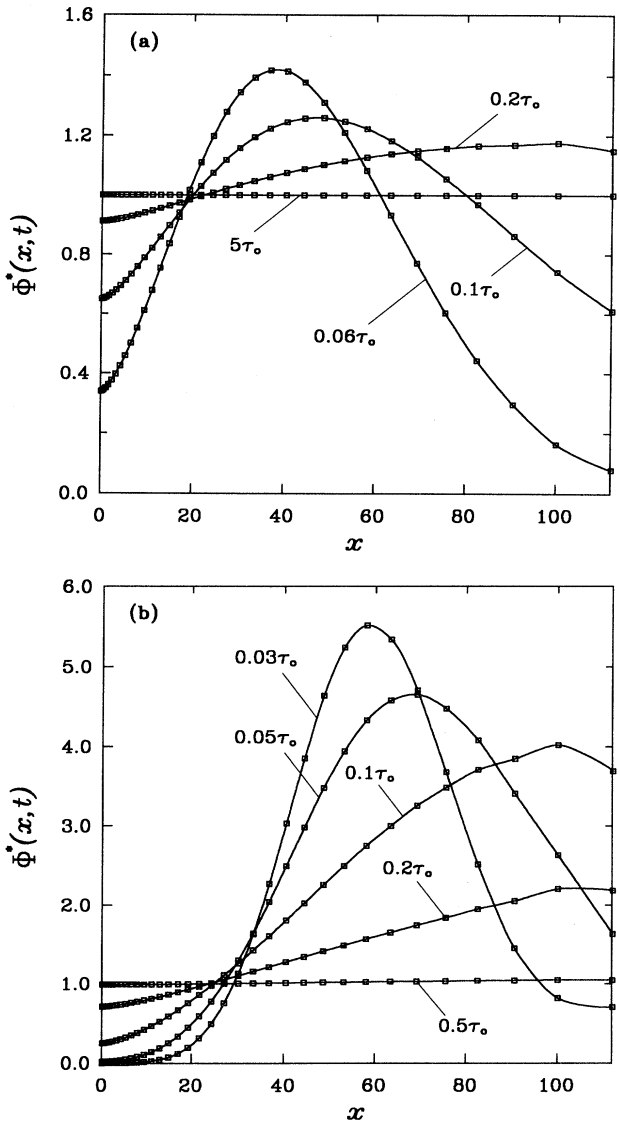

FIG. 3. Same as Fig. 2 for an electric field $E = 5 \times 10^4$ V/m: the initial peak is located at (a) $x \doteq 30$; (b) $x \doteq 49$.

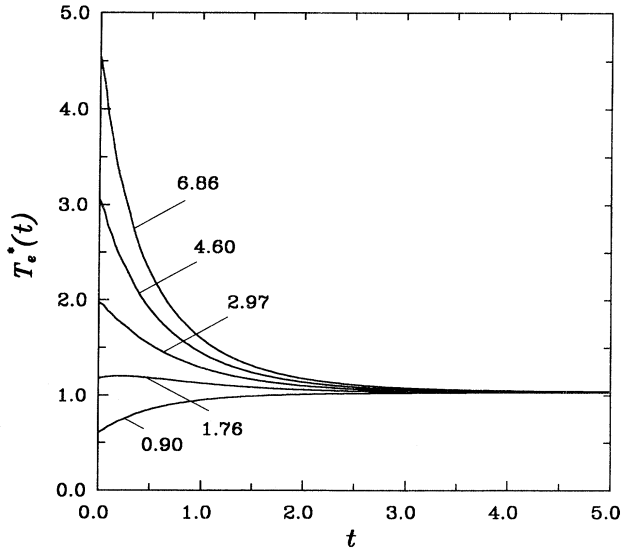

FIG. 4. Decay of the electron temperature $T_e^*(t) = T_e(t)/T_0$ for initial conditions $x \doteq 0.90$, 1.76, 2.97, 4.60, and 6.86 at $T_0 = 100$ K with $E = 5 \times 10^2$ V/m; the steady temperature is $T_e^*(\infty) \doteq 1.03$.

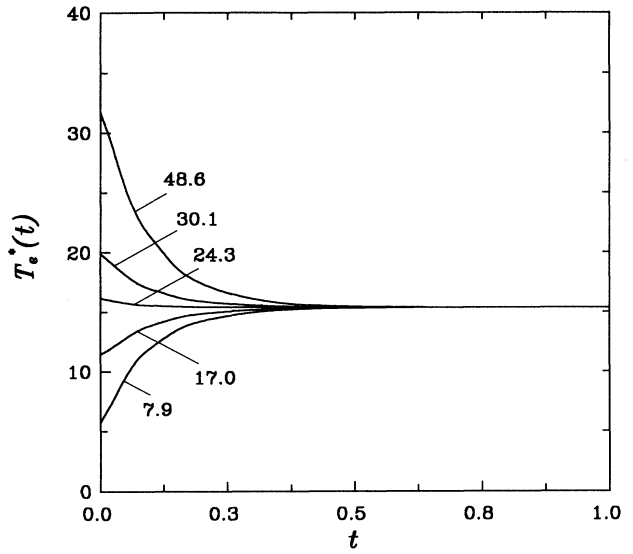

FIG. 5. Same as Fig. 4 for another field of $E = 5 \times 10^4$ V/m with initial conditions $x \doteq 7.9$, 17.0, 24.3, 30.1, and 48.6; the steady temperature is $T_e^*(\infty) \doteq 15.4$.

that corresponds to $T_e^*(0) \doteq 3.1$; in evaluating the results $N = 15$, 19, 21, 25, and 29 were used for fields $E = 5.0\times10^2$, 5.1×10^3, 1.0×10^4, 3.7×10^4, and 5.0×10^4 V/m, respectively. It shows a tendency that the electron temperature approaches a steady-state value faster when the applied field is stronger. For the high fields the electron temperature increases sharply in an initial short time. This is because electrons accelerate quickly and thus gain energies from the field before having a chance to emit phonons. This sharply increasing feature of electron temperature diminishes as the magnitude of fields decreases. For the low fields the temperature decays gradually until it reaches the steady value.

It is useful to characterize the decay of the electron temperature in terms of the relevant relaxation time which can be defined in a variety of ways. Here, we define an effective transient energy-relaxation time $\tau(t)$ as is done in the work of Kim and Shizgal[39] through

$$\frac{\partial T_e^*(t)}{\partial t} = -\frac{T_e^*(t) - T_e^*(\infty)}{\tau(t)} , \tag{55}$$

which brings out, with the help of Eq. (53),

$$\tau(t) = \frac{\sum_{\mu=1}^{N-1} \alpha_\mu \exp(-\lambda_\mu t)}{\sum_{\mu=1}^{N-1} \alpha_\mu \lambda_\mu \exp(-\lambda_\mu t)} . \tag{56}$$

The time variation of $\tau(t)$ is depicted in Fig. 7 with $E = 5.0 \times 10^3$ V/m for several initial excitation conditions. It manifests that the relaxation time tends to a constant after an initial transient time, whose value is seen to approach $1/\lambda_1$, which equals $0.33\tau_0 \doteq 0.19$ nsec in this case. This observation can be understood by taking a long-time limit of Eq. (56) such that

$$\tau(t) \to \frac{1}{\lambda_1} + \frac{\alpha_2}{\alpha_1 \lambda_1} \exp\{-(\lambda_2 - \lambda_1)t\} , \tag{57}$$

where $\lambda_1 < \lambda_2$. Thus, when the eigenvalue spectrum of the BFP operator is at least partially discrete, which is the case of our results, the average electron energy decays exponentially in the long-time limit and the relaxation can be characterized by the smallest nonzero dis-

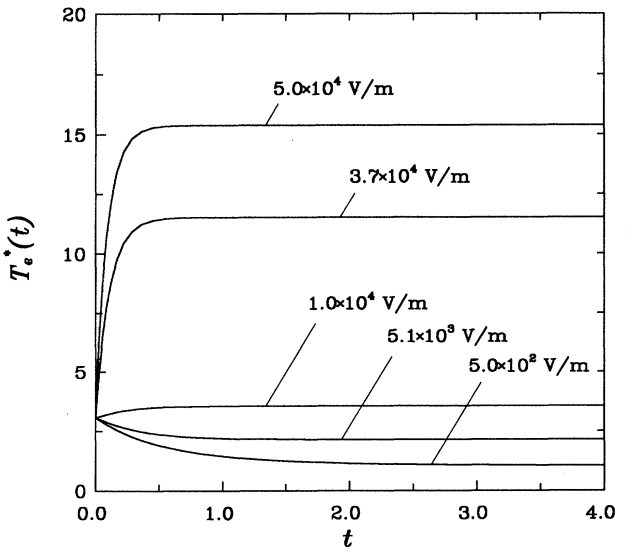

FIG. 6. Same as Fig. 4 but with a fixed initial condition $x \doteq 4.6$ for various electric fields $E = 5.0\times10^2$, 5.1×10^3, 1.0×10^4, 3.7×10^4, and 5.0×10^4 V/m.

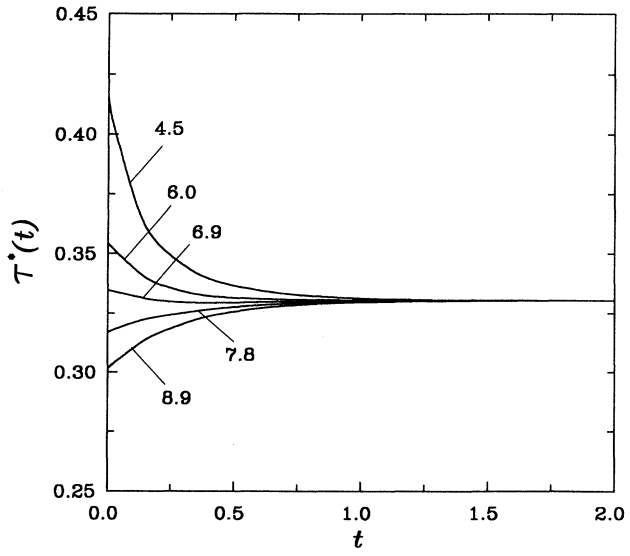

FIG. 7. Time variation of the transient energy relaxation time $\tau(t)$ for $E = 5.0 \times 10^3$ V/m with initial conditions $x \doteq 4.5$, 6.0, 6.9, 7.8, and 8.9.

crete eigenvalue λ_1. While the initial transient occurs, the temporal behavior of the decay would be more intricate so that there may exist more than two relaxation times at a certain stage and that it would be nonexponential in a shorter time scale in general. In Fig. 8 the normalized relaxation time, $\tau^*(t) \equiv \tau(t)/\lambda_1^{-1}$, is presented for various applied fields. Clearly, it is manifested that the relaxation time approaches a constant $1/\lambda_1$ for a given field after a sufficiently long time. For the higher fields the long-time characteristic of exponential decay of average energy is established faster compared to the lower-field cases. The complicated structures which appear in a very short time ($\leq 0.1\tau_0$) are not important because phenomena which appear in such a short-time regime are out of the scope of the Boltzmann transport theory.

In a recent work a formula for a temperature relaxation rate for metallic systems was derived by Allen. Allen's Eqs. (1) and (2) in Ref. 40 are equivalent to our Eq. (1) for nondegenerate electrons in the zero-field case and also when one neglects hot phonon effects by assuming N_Q as the Planck distribution function with the equilibrium temperature in it. Then, the emphasized parameter $\lambda\langle\omega^2\rangle$ in the reference is related to our energy-relaxation time $\tau(t)$ as

$$\lambda\langle\omega^2\rangle = \frac{\pi k_B T_e(t)}{3\hbar}\tau^{-1}(t).$$

The estimated numerical values for a peak temperature $T_e^*(0) \doteq 2.9$ are $\lambda\langle\omega^2\rangle \doteq 4.4 \times 10^{22}/\text{sec}^2 \approx 1.9 \times 10^{-2}$ meV^2 ($\hbar \equiv 1$) at $t = 1$ and $\lambda\langle\omega^2\rangle \doteq 2.8 \times 10^{22}/\text{sec}^2 \approx 1.2 \times 10^{-2}$ meV^2 at $t = 5$. However, one should notice that there exists an essential difference between two calculations: Allen used the thermal distribution function with the time-dependent temperature in it. On the other hand, our calculation obtains the athermal distribution function by solving the Boltzmann equation and then evaluating the time-dependent temperature.

The time-dependent drift velocity v_d which is defined to be the average velocity of electrons over the distribution function is calculated as

$$v_d(t) = v_0 \frac{N_c}{n} s \int_0^\infty dx' x' \frac{\partial f^{(0)}(sx',t)}{\partial x'} , \quad (58)$$

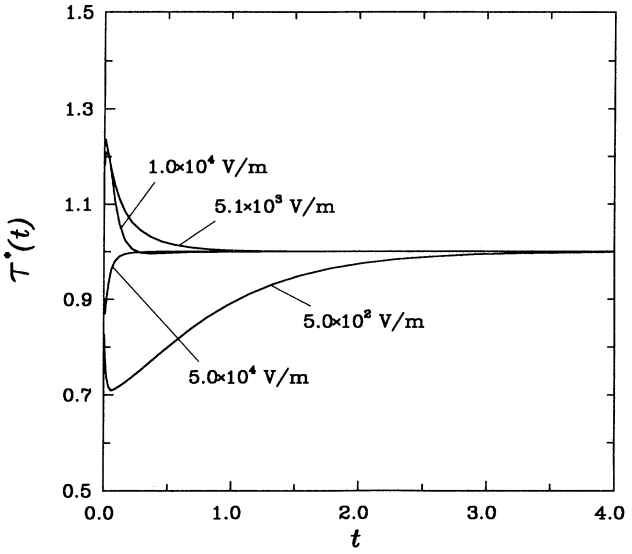

FIG. 8. Temporal behavior of the normalized energy relaxation time $\tau^*(t) = \tau(t)/\lambda_1^{-1}$ with a fixed initial condition $x \doteq 4.6$ for various electric fields $E = 5.0 \times 10^2$, 5.1×10^3, 1.0×10^4, and 5.0×10^4 V/m where the corresponding $\lambda_1^{-1} \doteq 0.46$, 0.19, 0.13, and 0.06 nsec for each field, respectively.

where n is the density of pumped electrons and the constant $v_0 = 2\sqrt{2}eEl_{ac}/\left(3\sqrt{m\pi k_B T_0}\right)$. Then, the field-dependent transient mobility can also be calculated from

$$\mu(t) \equiv \frac{1}{E} \mid v_d(t) \mid = \mu_0 \frac{N_c}{n} s \int_0^\infty dx' f^{(0)}(sx',t) , \quad (59)$$

where μ_0 is the zero-field mobility defined as $\mu_0 \equiv v_d(E \to 0)/E$. Here, we report the transient mobility normalized with respect to the zero-field mobility, which is calculated from

$$\mu^*(t) = \mu(t)/\mu_0 = \mu^*(\infty) + \sum_{\mu=1}^{N-1} \beta_\mu \exp(-\lambda_\mu t) , \quad (60)$$

where

$$\beta_\mu = \frac{\sqrt{\pi}}{2\sqrt{s}} \frac{\sum_{l=0}^{N-1} \left\{\chi_l \xi_l^{-3/2} (s\xi_l/\alpha + 1)^\alpha e^{(1-s)\xi_l}\right\}^{1/2} \Psi_l^{(\mu)} \Psi_m^{(\mu)}}{\sum_{l=0}^{N-1} \left\{\chi_l \xi_l^{-1/2} (s\xi_l/\alpha + 1)^\alpha e^{(1-s)\xi_l}\right\}^{1/2} \Psi_l^{(0)} \Psi_m^{(0)}} . \quad (61)$$

In Fig. 9 the normalized transient mobilities $\mu^*(t)$ are demonstrated for a field of $E = 5.0 \times 10^3$ V/m under several excitation conditions. Interestingly, the mobility of electrons that are excited at low energies increases for a short period of time and then decreases gradually to the steady-state value of $\mu^*(\infty) \doteq 0.63$. On the other hand, the mobilities of electrons that are injected at high energies increase monotonously until they saturate to the steady state. In Fig. 10 the time-dependent mobilities are drawn for various field strengths with a fixed initial excitation condition $x \doteq 4.6$. The mobility grows slowly for low fields until it reaches the steady state. As the field

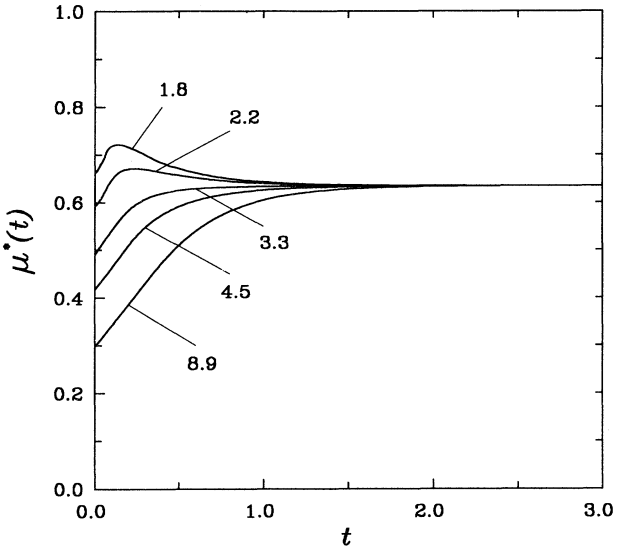

FIG. 9. Transient mobility of electrons $\mu^*(t) = \mu(t)/\mu_0$ where $\mu_0 = 3 \times 10^4$ cm^2/(V sec) for an electric field $E = 5.0 \times 10^3$ V/m with various initial conditions $x \doteq 1.8$, 2.2, 3.3, 4.5, and 8.9; the steady mobility $\mu^*(\infty)$ equals 0.63.

increases the temporal tendency is changed from growth to decay. For high fields the mobility decays quickly and transits to the steady state faster than low-field cases. Also, the steady mobility is seen to get smaller as the field increases, for instance, $\mu^*(\infty) \doteq 0.97$ for $E = 5.0 \times 10^2$ V/m but $\mu^*(\infty) \doteq 0.48$ for $E = 1.0 \times 10^4$ V/m. Similar to the energy-relaxation time, one may define the mobility decay time as

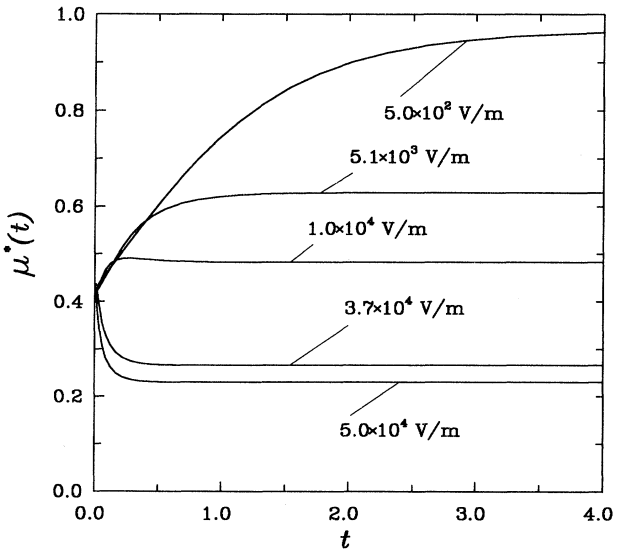

FIG. 10. Same as Fig. 9 with a fixed initial condition $x \doteq 4.6$ for various electric fields $E = 5.0 \times 10^2$, 5.1×10^3, 1.0×10^4, 3.7×10^4, and 5.0×10^4 V/m.

TABLE II. Hot electron temperature and mobility vs electric fields in the steady state where E is in units of V/m, the temperature is normalized by $T_0 = 100$ K, and the mobility is normalized with respect to $\mu_0 = 3 \times 10^4$ cm^2/(V sec).

E	$T_e^*(\infty)$	$\mu^*(\infty)$
1.0[+1][a]	1.00	0.995
5.0[+1]	1.00	0.995
1.0[+2]	1.00	0.994
5.0[+2]	1.03	0.973
1.0[+3]	1.10	0.927
5.0[+3]	2.12	0.635
1.0[+4]	3.56	0.483
5.0[+4]	15.4	0.230
1.0[+5]	30.2	0.164

[a] $[+n] \equiv 10^n$.

$$\tau_\mu(t) = \frac{\sum_{\mu=1}^{N-1} \beta_\mu \exp(-\lambda_\mu t)}{\sum_{\mu=1}^{N-1} \beta_\mu \lambda_\mu \exp(-\lambda_\mu t)}. \quad (62)$$

Again, the decay is exponential in the long-time limit and the corresponding effective constant relaxation time is characterized by the reciprocal of the smallest nonzero eigenvalue. On the other hand, the detailed time dependence of the initial transient would be different from that of the energy relaxation in general.

Finally, some of the calculated steady values of the hot electron temperature and mobility are reported in Table II. The stronger the magnitude of the applied field is, the hotter the steady value of the electron temperature is. Also, a clear manifestation of nonlinearity in the transport coefficient is seen: the value of the mobility deviates significantly from Ohm's law as the electric field is increased.

V. SUMMARY

The Legendre polynomial expansion has been a widely used method in obtaining an approximate analytical solution to the Boltzmann equation for studies of electrical transport in semiconductors under the influence of electric fields. Particularly, the two-term approximation is useful for nonpolar materials because in these materials it not only allows an accurate result for the carrier density, drift velocity, and electron temperature but also it represents the distribution function itself reasonably well. In the early investigations, however, most works were focused on the steady-state phenomena, for instance, the energy distribution functions and mobilities were obtained under steady-state conditions with respect to the applied electric field.

In this paper we have extended this approach to the time-dependent regime, and consequently the transient transport of charged carriers has been studied. The semiconductor considered as a model is a gas of nondegenerate conducting electrons that are excited by incoherent op-

tical pumping, limited by acoustic deformation potential scattering in an effective single parabolic and spherical energy band under the influence of external stationary electric fields. Consequently, the Boltzmann equation was converted into a more tractable differential equation, which was named the Boltzmann-Fokker-Planck equation, for the energy distribution function. The resultant equation was solved numerically under the general time-dependent situation for the pulsed initial conditions by utilizing a matrix method. The matrix method we used has been proven to be very efficient for a complicated transport calculation in the sense that a relatively small number of eigenfunctions is needed for the BFP operator to correctly produce an accurate distribution function. This method is analogous to the Gaussian quadrature rule in numerical integration, which produces a desirable accuracy while utilizing a small number of quadrature points optimally.

It is seen that the sharply peaked initial electron distribution broadens with time smoothly and eventually relaxes to the sedimentation nonequilibrium distribution, the well-known Davydov-Druyvesteyn distribution function, in the infinite-time limit. The condition of particle conservation was monitored in order to assure the numerical accuracy at each time. Subsequently, the macroscopic thermodynamic variables such as the hot electron temperature, drift velocity, and also the transport coefficients such as the mobility were evaluated by calculating relevant velocity moments over the distribution function obtained. The transient mobility approaches the steady-state value differently depending on initial conditions and magnitude of fields. Under a low excitation condition the mobility increases for a short period of time and then relaxes to the steady value. On the other hand, it increases monotonously until it saturates to the steady value for electrons that are excited at high energies. The mobility approaches the steady-state value faster when the applied field is bigger under the same excitation condition. Also, the results show that the steady mobility decreases as the magnitude of the field increases, which reflects deviations from the linear response. The electron temperature heats up under the low excitation conditions and cools down under the high excitation conditions before reaching the steady hot temperature for a chosen field. The electron temperature decays faster for a higher field compared to the result of a smaller field and the steady hot electron temperature becomes hotter as the strength of the applied field increases.

In addition, we have introduced the time-dependent relaxation time of the average electron energy and of mobility in order to analyze the transient behavior more quantitatively. The nature of the approach to the steady state has been discussed in terms of the eigenvalues of the BFP operator. The important aspects of our results are that the decay of electron temperature as well as mobility toward steady state is exponential in the long-time limit and that the corresponding relaxation time is characterized by a smallest nonzero eigenvalue of the BFP operator. In a shorter-time transient regime it is expected that the relaxation would be more complicated.

ACKNOWLEDGMENT

This research has been supported by the Ministry of Education through the Institute of Basic Sciences at Chonnam National University (Grant No. BSRI-94-2431).

*Author to whom all correspondence should be addressed.

[1]B. R. Nag, *Theory of Electrical Transport in Semiconductors* (Pergamon, Oxford, 1972).
[2]E. M. Conwell, *High Field Transport in Semiconductors* (Academic, New York, 1967), Suppl. 9.
[3]J. Yamashita and M. Watanabe, Prog. Theor. Phys. **12**, 443 (1954).
[4]I. B. Levinson, Fiz. Tverd. Tela. (Leningrad) **6**, 2113 (1964) [Sov. Phys. Solid State **6**, 1665 (1965)].
[5]C. Hammar, J. Phys. C **6**, 70 (1973).
[6]R. L. Liboff and G. K. Schenter, Phys. Rev. B **34**, 7063 (1986); G. K. Schenter and R. L. Liboff, J. Appl. Phys. **62**, 177 (1987); Phys. Rev. B **40**, 5624 (1989).
[7]S. M. Cho and H. H. Lee, J. Appl. Phys. **71**, 1298 (1992).
[8]B. A. Sanborn, P. B. Allen, and G. D. Mahan, Phys. Rev. B **46**, 15 123 (1992).
[9]G. Cavalleri and G. Mauri, Phys. Rev. B **49**, 9993 (1994).
[10]S. K. Sarker, Y.-K. Hu, C. J. Stanton, and J. W. Wilkins, Phys. Rev. B **35**, 9229 (1987).
[11]*Numerical Data and Functional Relationships in Science and Technology*, edited by O. Madelung, Landolt-Börnstein, New Series, Vol. 17, Pt. a (Springer-Verlag, New York, 1982).
[12]S. A. Lyon, J. Lumin. **35**, 121 (1986).
[13]J. L. Ouder, D. Hulin, A. Migus, A. Antonetti, and F. Alexandre, Phys. Rev. Lett. **55**, 2074 (1985).
[14]W. L. Lin, L. G. Fujimoto, E. P. Ippen, and R. A. Logan, Appl. Phys. Lett. **50**, 124 (1987); R. W. Schoenlein, W. Z. Lin, E. P. Ippen, and J. G. Fujimoto, *ibid.* **51**, 1442 (1987).
[15]W. H. Knox, *Hot Carriers in Semiconductor Nanostructures: Physics and Applications* (AT&T, Holmdel, NJ, 1992), p. 313.
[16]E. G. S. Paige, J. Phys. Chem. Solids **16**, 207 (1960); A. F. Gibson, J. W. Granville, and E. G. S. Paige, *ibid.* **19**, 198 (1961).
[17]A. Neukermans and G. S. Kino, Phys. Rev. B **7**, 2693 (1973).
[18]F. Nava, C. Canali, F. Catellani, G. Gavioli, and G. Ottaviani, J. Phys. C **9**, 1685 (1976).
[19]R. Y. Chen and D.-S. Pan, J. Appl. Phys. **70**, 4938 (1991).
[20]C. Jacoboni and L. Reggiani, Rev. Mod. Phys. **55**, 645 (1983).
[21]C. S. Kim, J. Korean Phys. Soc. **27**, 260 (1994).
[22]H. Risken, *The Fokker-Planck Equation* (Springer-Verlag, Berlin, 1989).
[23]J. P. Aubert, J. C. Vaissiere, and J. P. Nougier, J. Appl. Phys. **56**, 1128 (1984).
[24]S. Krishnamurthy, A. Sher, and A. B. Chen, Appl. Phys. Lett. **55**, 1002 (1989).
[25]Y. S. Sun and C. J. Stanton, Phys. Rev. B **43**, 2285 (1991).

[26]G. Blatter and F. Greuter, Phys. Rev. B **34**, 8555 (1986); G. Blatter and D. Baeriswyl, *ibid.* **36**, 6446 (1987).
[27]C. S. Kim and D. Y. Kim, J. Korean Phys. Soc. **26**, 343 (1993).
[28]J. Bardeen and W. Shockley, Phys. Rev. **80**, 72 (1950).
[29]M. Combescot and J. Bok, Phys. Rev. B **35**, 1181 (1987).
[30]D. S. Tang, Phys. Rev. B **36**, 2757 (1987).
[31]F. Capasso, in *Lightwave Communications Technology, Part D: Photodetectors*, edited by W. Tsang, Semiconductors and Semimetals Vol. 22 (Academic, San Diego, 1986), p. 1.
[32]H. H. K. Tang, Phys. Rev. B **46**, 6768 (1992).
[33]E. Bringuier, Phys. Rev. B **49**, 7974 (1994).
[34]D. Arnold, E. Cartier, and D. J. DiMaria, Phys. Rev. B **49**, 10 278 (1994).
[35]M. J. Druyvestyn, Physica **10**, 61 (1930).
[36]S. Buddhudu, W. E. Hagston, M. J. Swift, and A. J. Waring, J. Phys. C **21**, L725 (1988).
[37]K. Seeger, *Semiconductor Physics* (Springer-Verlag, New York, 1989).
[38]H. Hochstadt, *The Functions of Mathematical Physics* (Dover, New York, 1972).
[39]C. S. Kim and B. Shizgal, Phys. Rev. B **44**, 2969 (1991).
[40]P. B. Allen, Phys. Rev. Lett. **59**, 1460 (1987).